GENETICS

The macrophage genetic cassette *inr/dtor/pvf2* is a nutritional status checkpoint for developmental timing

Sergio Juarez-Carreño*† and Frederic Geissmann*

A small number of signaling molecules, used reiteratively, control differentiation programs, but the mechanisms that adapt developmental timing to environmental cues are less understood. We report here that a macrophage *inr/dtor/pvf2* genetic cassette is a developmental timing checkpoint in *Drosophila*, which either licenses or delays biosynthesis of the steroid hormone in the endocrine gland and metamorphosis according to the larval nutritional status. Insulin receptor/dTor signaling in macrophages is required and sufficient for production of the PDGF/VEGF family growth factor Pvf2, which turns on transcription of the sterol biosynthesis Halloween genes in the prothoracic gland via its receptor Pvr. In response to a starvation event or genetic manipulation, low Pvf2 signal delays steroid biosynthesis until it becomes Pvr-independent, thereby prolonging larval growth before pupariation. The significance of this developmental timing checkpoint for host fitness is illustrated by the observation that it regulates the size of the pupae and adult flies.

INTRODUCTION

Controlled developmental timing is essential for fitness in the plant and animal phyla, because it allows the success of critical transitions such as sexual reproduction through flowering in plants (*1*), puberty/sexual maturation in mammals (*2*, *3*), and metamorphosis from larvae to adults in insects (*4*, *5*). Puberty and metamorphosis are triggered by the production of steroid hormones in endocrine glands. In mammals, the hypothalamus gonadotropin-releasing hormone (GnRH) controls steroid synthesis via the anterior pituitary hormones: adrenocorticotropic hormone (ACTH), luteinizing hormone (LH), and follicle-stimulating hormone (FSH) (*2*, *3*, *6*). In *Drosophila*, the GnRH superfamily hormone corazonin (Crz), as well as AstA/AstaR (*7*) and Dilp8/Lgr3 (*8*–*10*), controls steroid synthesis via the prothoracicotropic hormone (PTTH) produced by the PTTH neurons (*4*, *11*–*13*). Although genetic and molecular studies have identified the limited number of conserved signaling molecules that are used reiteratively to control puberty, metamorphosis, and, more generally, differentiation (*14*), the mechanisms that adapt developmental timing to external cues are less understood. Nutritional status is an important factor that can delay development, when suboptimal nutrition could compromise the fitness of the adult. Specifically, the production of fat-derived signals acting on the brain, such as leptin in mammals and its *Drosophila* ortholog Upd2, with Eiger and Stu, represents critical checkpoints for nutritional status that control puberty and metamorphosis (*12*, *15*–*21*). The developmental timing of puberty and metamorphosis, therefore, integrates nutritional quality control checkpoints, which rely on interorgan communication networks, to optimize the timing of steroid hormone synthesis and the fitness of adults. However, these interorgan and intercellular communication networks remain poorly understood. Macrophages are accessory cells present throughout tissues, and recent findings have attracted attention to their roles in developmental processes, interorgan communication, and metabolism including in response to nutrient availability (*22*–*28*) and steroid hormone synthesis (*29*, *30*). Moreover, macrophage deficiency delays metamorphosis in *Drosophila* (*31*) and impairs steroid hormone synthesis and sexual maturation of rodents (*27*, *32*–*41*) and may thus contribute to developmental checkpoints. Therefore, we took advantage in this work of the strong genetically tractability at the organismal level of *Drosophila melanogaster* to investigate the mechanisms that may allow macrophages to regulate steroid hormone production and developmental growth.

RESULTS

Starvation and macrophage deficiency delay ecdysone biosynthesis and metamorphosis in *Drosophila* larvae

Drosophila larvae lacking nutrients at the pre–critical weight (pre-CW) phase (fig. S1A) and hemolectin (hml)–expressing macrophages both display a developmental delay in the onset of metamorphosis also known as the larva-to-pupa transition or pupariation (*31*, *42*, *43*). Pupariation of larvae starved at the pre-CW phase, 88 hours after egg laying (AEL), for a period of 8 hours (see Materials and Methods and fig. S1A) was delayed by ~8 hours in comparison to controls fed on standard molasses medium (Fig. 1A). Delayed pupariation of larvae starved at the pre-CW phase is due to delayed ecdysone biosynthesis by the prothoracic gland (fig. S1B) (*42*, *43*). Accordingly, at the time of the normal onset of pupariation under our laboratory conditions (104 hours AEL), transcription of the ecdysone target *eip75b* (*e75b*) (Fig. 1B) (*44*) and ecdysone levels (Fig. 1C) were reduced by ~90% in comparison to control. Macrophage-less larvae (Fig. 1C) (*27*, *45*, *46*) also presented with an ~8-hour delayed pupariation, but irrespectively of feeding conditions (fig. S1A and Fig. 1, D and E). A time course analysis indicated that transcription of the ecdysone target *eip75b* in these conditions is delayed by ~8 hours in comparison to controls (Fig. 1F), and ecdysone levels are reduced by ~90% at 104 hours AEL (Fig. 1G). Transcription of the ecdysone biosynthetic enzymes (*47*)—*neverland* (*nvd*), *phantom* (*phm*), and *shadow* (*sad*)—was also delayed by ~8 hours (Fig. 1H) as observed in starved larvae (fig. S1B). These data suggested that both pre-CW

Immunology Program, Sloan Kettering Institute, MSKCC, New York, NY 10065, USA.
*Corresponding author. Email: sergio.juarez@irbbarcelona.org (S.J.-C); geissmaf@mskcc.org (F.G.)
†Present address: Institute for Research in Biomedicine (IRBBarcelona), The Barcelona Institute of Science and Technology, BaldiriReixac, 10, 08028 Barcelona, Spain.

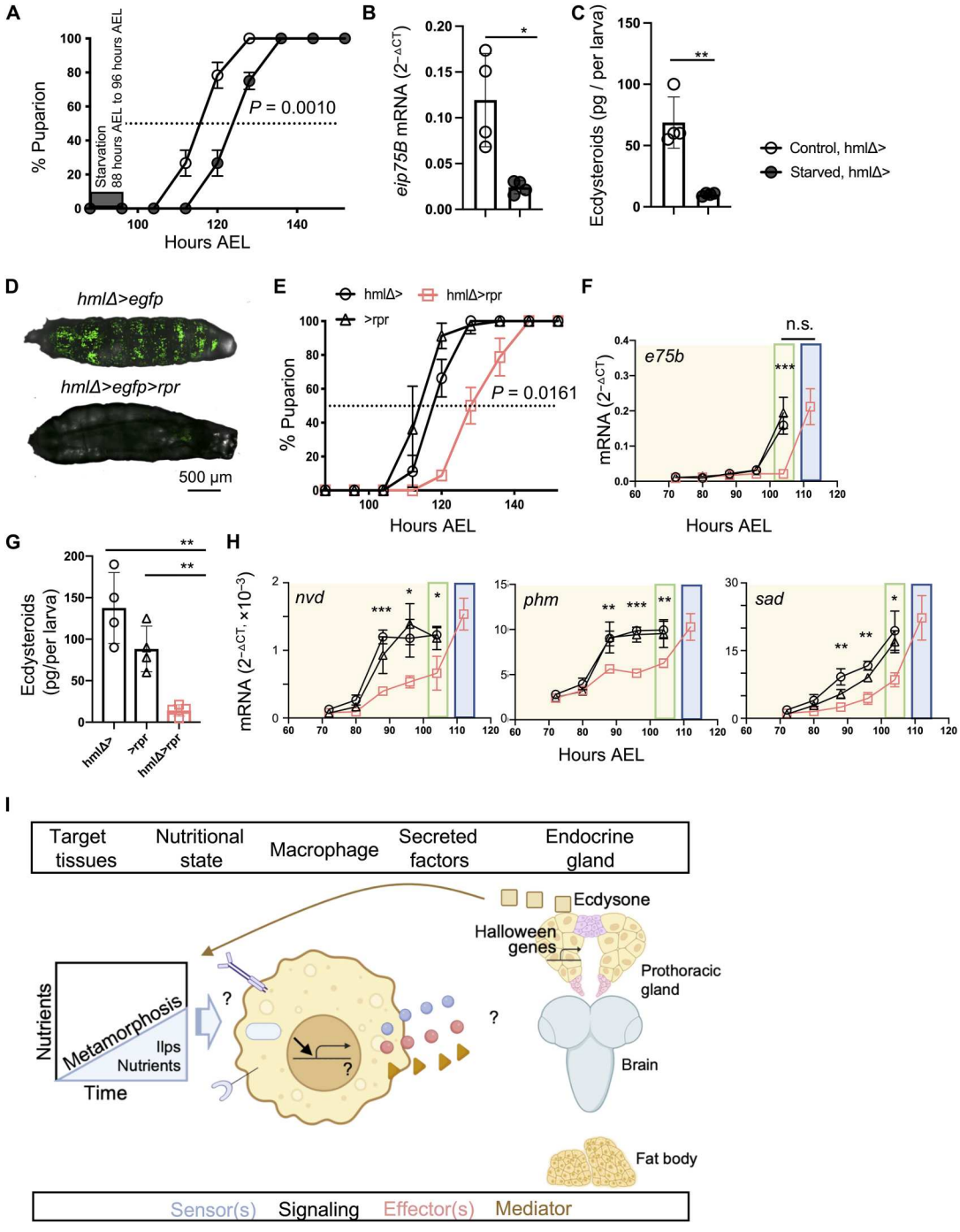

Fig. 1. Nutrient deprivation and macrophages-less larvae display a developmental delay from ecdysone synthesis inhibition. (**A**) Developmental timing in larvae under starvation treatment for 8 hours at 88 hours AEL. (n = 3, 20 larvae per genotype in three independent crosses, 60 larvae in total per condition). (**B**) Transcriptional levels of the ecdysone signaling target gene *eip75b* in starved flies. mRNA levels normalized to *rp49* at 104 hours AEL. n = 4. Samples were pooled by five larvae per condition and genotype. (**C**) Total ecdysone levels in whole larvae under starvation treatment for 8 hours at 88 hours AEL in the indicate genotypes, quantified by enzyme-linked immunosorbent assay (ELISA) at 104 hours AEL. n = 4, each sample pooled of 10 larvae. (**D**) Confocal imaging of larvae with GFP fluorescent macrophages and larvae depleted for macrophages. (**E**) Developmental timing in larvae depleted of macrophages (n = 3, 20 larvae per genotype in three independent crosses, 60 larvae in total per condition). (**F**) mRNA levels of the ecdysone signaling target gene *eip75b* in macrophage-less larvae. mRNA levels are normalized to *rp49* at different time points in larva lacking macrophages. n = 3, each sample pooled of five larvae. (**G**) Ecdysone levels in macrophage-less larvae, quantified by ELISA at 104 hours AEL. n = 4, each sample pooled of 10 larvae. (**H**) mRNA levels of the Halloween genes *nvd*, *phm*, and *sad* in macrophage-less larvae. mRNA levels are normalized to *rp49* at different time points. n = 3, each sample five pooled larvae. Green boxes represent the normal developmental timing in control conditions, and blue boxes represent the developmental delay in experimental conditions. (**I**) Working model of ecdysone synthesis regulation by nutrient-sensing receptors and secreted factors present in macrophages during development. Scheme created with BioRender.com. Statistical analysis: two-tailed unpaired t test; values represent the means ± SD. $^*P < 0.05$, $^{**}P < 0.01$, and $^{***}P < 0.001$; n.s. not significant.

starvation and macrophage deficiency increase the length of the L3 larval (feeding) stage before pupariation by delaying the biosynthesis of ecdysone. Macrophages can act as nutrient sensors (*22*), and we therefore considered the hypothesis that they may regulate ecdysone biosynthesis to optimize the timing of pupariation according to the nutritional status of the larvae (Fig. 1I). To test this hypothesis, we performed genetic screens to identify the putative macrophage secreted growth factor(s) or cytokines that could directly or indirectly control developmental timing via ecdysone synthesis, along with the putative sensor(s) for larval nutritional status that could regulate the production of the secreted factor(s) by macrophages.

Production of the PDGF family member *pvf2* by macrophages controls the timing of ecdysone production and metamorphosis

Drosophila macrophages express nutritional sensors, such as nuclear receptors and the insulin receptor (InR), and are a source of secreted factors including cytokines and growth factors that can mediate adaptive responses of local or distant tissues in response to external or internal cues (*27*, *28*, *48*). We thus designed a targeted knockdown screen for genes encoding secreted factors and nutrient-sensing receptors that are expressed in larval macrophages before the onset of pupariation (96 hours AEL) (figs. S2 and S3) (*49*), testing their role in the timing of pupariation and ecdysone production. We found that selective knockdown of the platelet-derived growth factor (PDGF)/vascular endothelial growth factor (VEGF) conserved secreted factor *pvf2* in macrophages, using three independent RNA interference (RNAi) transgenes and three hemocyte drivers recapitulated the ~8-hour delay in pupariation (Fig. 2, A to C, and fig. S4, A to C). Pupariation was also delayed in the $pvf2^{c06947}$ loss-of-function mutant ($pvf2^{-/-}$) (Fig. 2B and fig. S4D) (*50*). Nevertheless, knockdown of *pvf2* in other tissues such as the fat body, prothoracic gland, trachea system, and glia cells did not affect pupariation (Fig. 2B and fig. S4E). In addition, we found that *pvf2* transcript levels were selectively low in larvae deficient in macrophages (Fig. 2D) and in macrophages from starved larvae (Fig. 2E and fig. S4F). Furthermore, knockdown of *pvf2* in macrophages delayed transcription of the ecdysone target *eip75b* (Fig. 2F) and reduced ecdysone production at 104 hours AEL (Fig. 2G), as observed in macrophage-less and starved larvae. Conversely, supplementation with the active form of ecdysone hormone, 20-hydroxyecdysone (20-HE; 0.5 mg/ml in food), rescued the developmental delay of larvae lacking *pvf2* in macrophages and macrophages-less larvae (fig. S4G). Last, expression of a *pvf2* transgene in macrophages also fully rescued the developmental delay and ecdysone production in starved larvae (Fig. 2, H and I) as well as in the $pvf2^{-/-}$ mutant (Fig. 2, J and K), although it did not trigger early pupariation before 104 hours AEL (Fig. 2, H and J). Together, these data indicate that transcriptionally regulated production of Pvf2 by macrophages controls an 8-hour window in the timing of ecdysone production and metamorphosis, based on whether the larvae have eaten. This suggests that the production of Pvf2 by macrophages is a nutritional status checkpoint for the developmental timing of metamorphosis.

Insulin/TOR signaling is required for of *Pvf2* production by macrophages

While testing the effect of known molecular sensors of nutritional status, we found that knockdown in larval macrophages of the *insulin-like receptor* (*inr*) (*51*) and *target of rapamycin* (*dtor*) (fig. S5A) (*52*), but not of the ecdysone receptor itself, also recapitulated the developmental delay observed in starved, macrophage-less, and macrophage-*pvf2*–deficient larvae (Fig. 2, L and M, and fig. S3). The insulin/target of rapamycin (TOR) pathway is a conserved sensor of nutritional stress in metazoans, controlling cell and organism growth (*53*–*55*) and particularly the timing of differentiation (*14*). The array of nutrition-related signaling inputs to this pathway has been defined (*56*), but the growth-regulatory outputs are less clear. Overexpression of a dominant-negative *inr* ($uas\text{-}inr^{DN}$) in macrophages or a second independent *dtor* RNAi line recapitulated the pupariation delay (fig. S5, B and C). In addition, macrophage *inr* and *dtor* knockdown both specifically decreased *pvf2* expression (Fig. 2N and fig. S5D), ecdysone production (Fig. 2O), and transcription of *eip75b* (Fig. 2P). Moreover, we found that the epistatic rescue of *dtor* knockdown larvae by expression of a *pvf2* transgene in macrophages restored developmental timing (Fig. 2Q) and ecdysone production (Fig. 2R). Of note, InR can regulate metabolism and growth via two main downstream pathways: activation of Tor and inhibition of FoxO (*51*), but *FoxO* overexpression did not affect developmental timing (fig. S5E). These results indicate that the InR/TOR pathway in macrophages regulates ecdysone production and the developmental timing of pupariation via the production of Pvf2.

Macrophage-derived *Pvf2* regulates ecdysone biosynthesis via its receptor *Pvr* in the prothoracic gland

Together, the above data identify an *inr*/*dtor*/*pvf2* macrophage genetic cassette that acts as a nutritional status checkpoint that can delay ecdysone production. Ecdysone is mainly produced by the prothoracic gland, an endocrine gland in the *Drosophila* larva (*12*). As noted above, ecdysone production in the prothoracic gland is under the control of the *Drosophila* GnRH superfamily hormone Crz-producing neurons, via the PTTH produced by the PTTH neurons, and of *Drosophila* insulin-like peptides (DILPs) produced by insulin-producing neurons (*4*, *5*, *11*–*13*). However, tyrosine kinase receptors including Pvr can also regulate developmental timing (*57*). Pvr is the only known Pvf receptor in *Drosophila* (*58*) and is expressed ubiquitously by macrophages, neurons, and fat body cells (*59*, *60*). Thus, we next investigated whether macrophage Pvf2 may control ecdysone synthesis in the prothoracic gland directly or indirectly through its effect on macrophages themselves, neurons, or fat body cells.

A time course analysis of Pvr expression in the prothoracic gland using an anti-Pvr antibody indicated that Pvr is first detected at 88 hours AEL and stays detectable until the onset of maturation at 104 hours AEL (Fig. 3A). Consistently, we found that transcription of *pvr* in dissected brain/ring gland tissue was up-regulated between 80 and 88 hours AEL to reach its highest level at 104 hours AEL (Fig. 3B). Furthermore knockdown of *pvr* in the prothoracic gland recapitulated the 8-hour developmental delay observed in starved; macrophage-less; and *pvf2*-, *inr*-, and *dtor*-knockdown models above (Fig. 3C and fig. S6A). The hypomorphic pvr^{01} mutant (*58*) recapitulated the developmental delay (fig. S6B). Knockdown of *pvr* in fat body, neurons, or macrophages did not affect the developmental timing (Fig. 3D and fig. S6C). In contrast, knockdown of *pvr* in the prothoracic gland did decrease ecdysone synthesis at 104 hours AEL (Fig. 3E) and delayed transcription of the target gene *eip75b* by 8 hours (Fig. 3F). As observed in the starved and macrophage-less *inr* and *dtor* models (see Fig. 1G and figs. S1B and S6D), we found that knockdown of *pvf2* in macrophages and knockdown of *pvr* in the prothoracic gland delayed transcription of the ecdysone biosynthetic pathway genes *nvd*, *phm*, and *sad* by 8 hours (Fig. 3G). In contrast, starvation or *inr* and *dtor* knockdown did not decrease *pvr* levels in the brain–ring gland complex (Fig. 3H and fig. S6E). Last, *pvr* overexpression in the prothoracic gland (*57*) fully rescued and even accelerated the developmental timing and ecdysone production in the $pvf2^{-/-}$ mutant (Fig. 3, I and J, and fig. S6, F and G). Of note, the latter contrasts with *pvf2* overexpression that did not accelerate the developmental timing (Fig. 2, H and J, and fig. S6H). We also examined a possible redundancy between the role of Pvf2 and its paralogs Pvf1 and Pvf3,

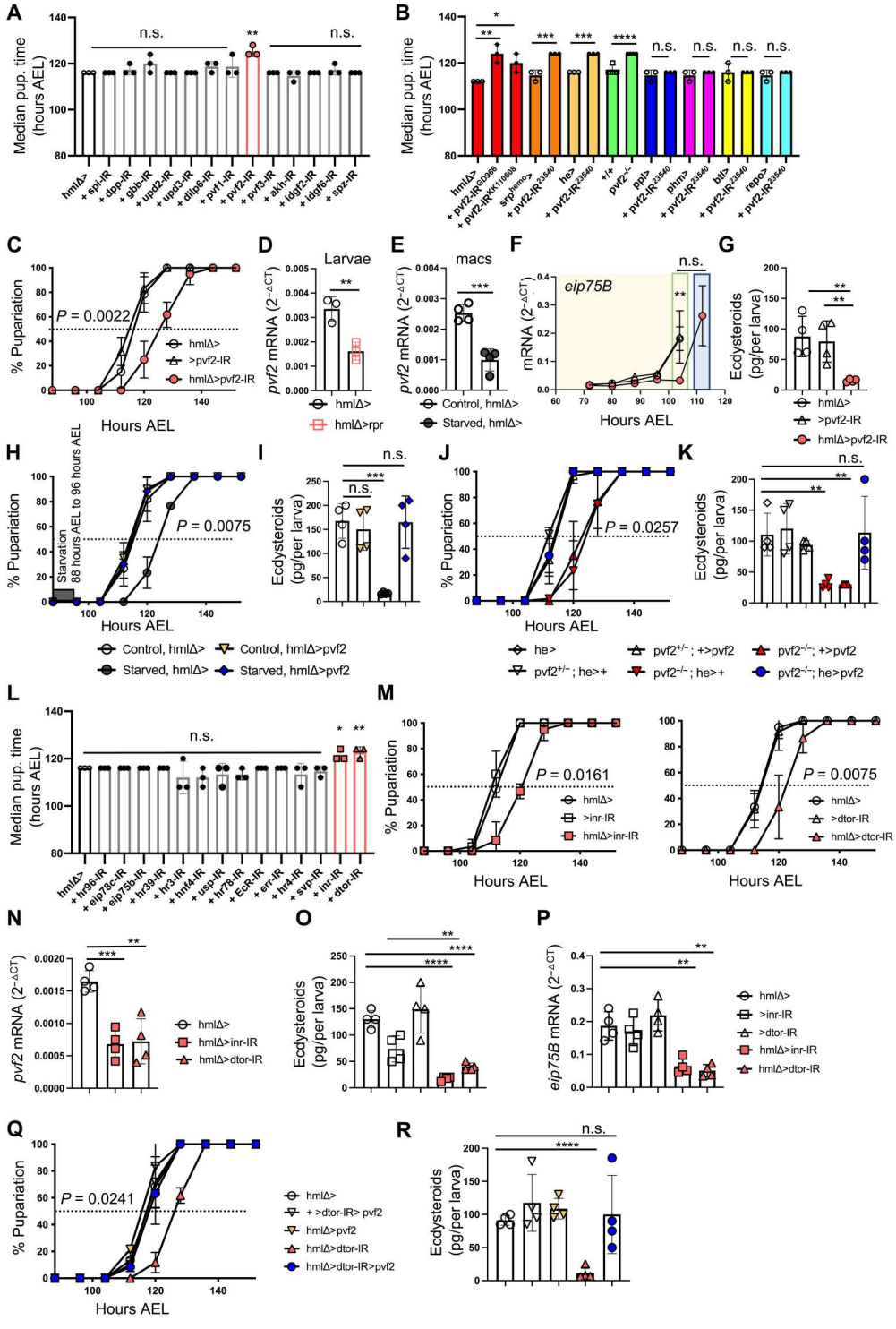

Fig. 2. A genetic screen in macrophages identifies a *inr/dtor/pvf2* cassette that controls pupariation and ecdysone synthesis under nutritional availability. (**A**) Median time of pupariation of the secreted factors in RNA interference (RNAi) screen. (**B**) Median time of pupariation in *pvf2* depletion in different tissues. (**C**) Lacking *pvf2* in macrophages induces developmental delay. (**D**) *pvf2* mRNA levels of macrophage-less larvae. (**E**) *pvf2* mRNA levels of 20000 macrophages in starved larvae. $n = 3$ to 4 at 96 hours AEL. (**F**) Transcriptional levels of *eip75b* in *pvf2* depleted macrophage larvae. $n = 3$. Samples were pooled by five larvae per condition. (**G**) Ecdysone levels in *pvf2* depleted macrophage larvae. (**H**) Developmental timing rescue by overexpression of *pvf2* in starved flies. (**I**) Ecdysone levels in starved larvae rescued by *pvf2* overexpression. (**J**) Developmental timing rescue of $pvf2^{c0694}$ mutant by *pvf2* overexpression. (**K**) Ecdysone total levels rescue in $pvf2^{c0694}$ mutant by *pvf2* overexpression. (**L**) Median time of pupariation of the nutrient-sensing receptors in RNAi screen. (**M**) Knockdown of *inr* and *dtor* in macrophages induces developmental delay. (**N**) mRNA levels of *pvf2* from 20,000 macrophages at 96 hours AEL. $n = 4$. (**O**) Ecdysone total levels in larvae of the indicate genotype. (**P**) Transcriptional levels of *eip75b* in flies of the indicate genotypes at 104 hours AEL. $n = 4$. (**Q**) Developmental timing rescue in *dtor*-lacking macrophages mutant by *pvf2* overexpression. (**R**) Ecdysone total levels in whole larvae in the indicate genotypes. For developmental timing experiments, $n = 3$, 20 larvae per genotype in three independent crosses, 60 larvae in total per condition. For quantification of ecdysone, $n = 4$, each sample was 10 larvae of the indicated genotypes at 104 hours AEL. mRNA levels were normalized to *rp49* in RT-qPCR. Data were analyzed by two-tailed unpaired *t* test, and values represent the means ± SD. *$P < 0.05$, **$P < 0.01$, ***$P < 0.001$, and ****$P < 0.0001$.

as they share the same receptor Pvr (*58*). However, starvation and *inr* and *dtor* knockdown did not alter *pvf1* and *pvf3* transcript levels (figs. S4F and S5C). In addition, knockdown of *pvf1* and *pvf3* did not affect developmental timing or ecdysone synthesis (Fig. 2A and figs. S2D and S7). Together, these data indicate that InR/dTor signaling in macrophages is required for Pvf2 production, which is, in turn, required to trigger pupariation at 104 hours AEL, by acting on its receptor Pvr, expressed in the prothoracic gland at the onset of pupariation to initiate ecdysone synthesis. However, these data also reveal that, in the absence of the Pvr-dependent signaling axis, which we describe here, ecdysone biosynthesis and pupariation are initiated 8 hours later in a Pvr-independent manner.

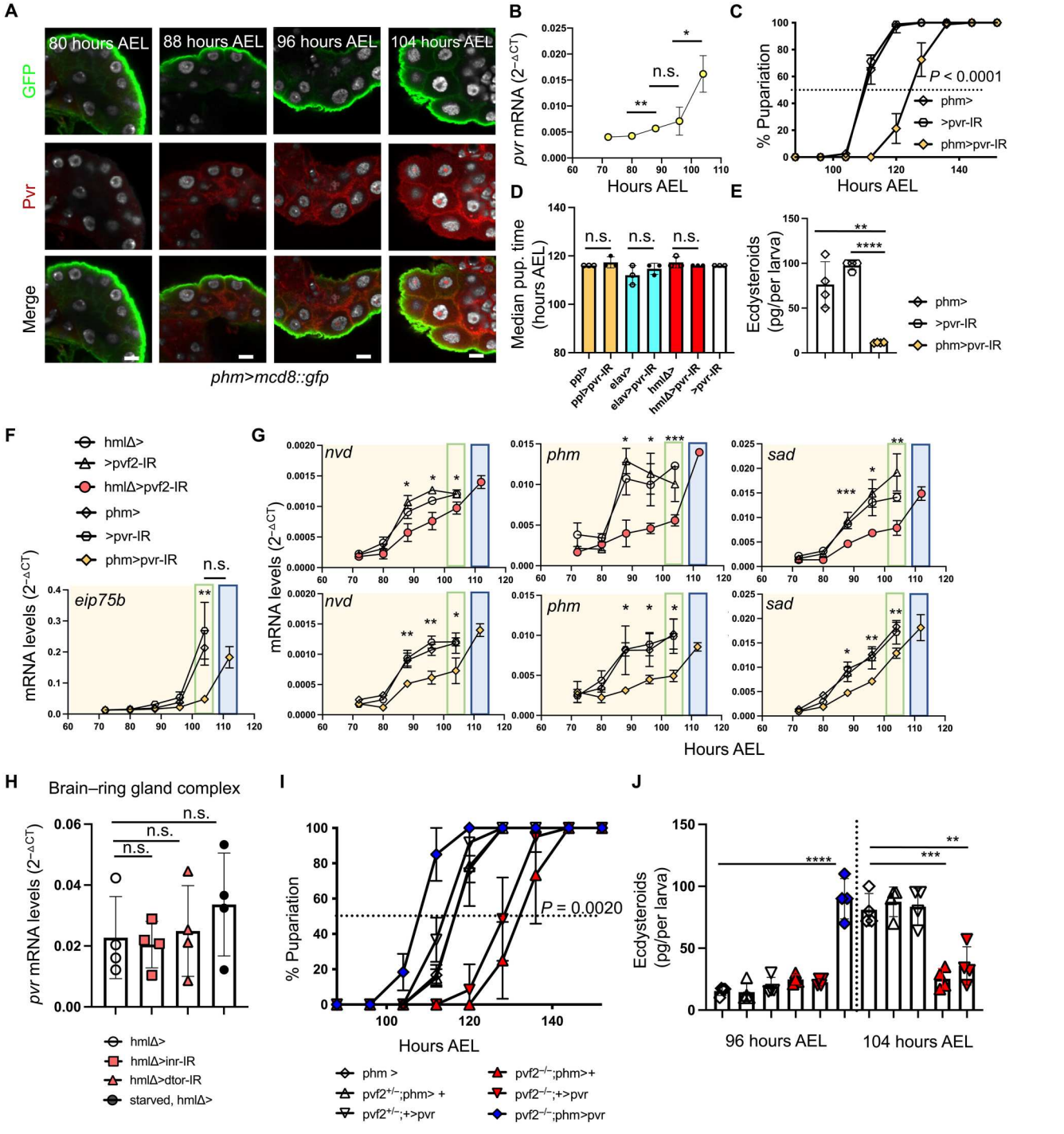

Fig. 3. Macrophage-derived Pvf2 acts through its receptor Pvr in the prothoracic gland to control ecdysone synthesis. (**A**) Pvr expression pattern in prothoracic gland at different time points indicated. Scale bars, 20 μm. $n = 4$ to 7. (**B**) *pvr* transcriptional levels. mRNA levels are normalized to *rp49*. $n = 3$. (**C**) Knockdown of *pvr* in the prothoracic gland induces developmental delay. (**D**) Median time of pupariation in *pvr* knockdown in fat body, neurons, and macrophages. (**E**) Total ecdysone levels in the indicate genotype at 104 hours AEL, quantified by ELISA. (**F**) Ecdysone target gene *e75b* mRNA levels normalized to *rp49* in larva lacking *pvr* in prothoracic gland. $n = 3$, each sample pooled of five larvae of the indicated genotype. (**G**) mRNA levels of the *nvd*, *phm*, and *sad* genes in larvae with *pvf2* depletion in macrophages or *pvr* depletion in prothoracic gland. mRNA levels are normalized to *rp49*. $n = 3$, each sample pooled of five larvae. Green boxes represent the normal developmental timing in control conditions, and blue boxes represent the developmental delay in experimental conditions. (**H**) mRNA levels of *pvr* in brain–ring gland complex of the indicated genotypes. mRNA levels are normalized to *rp49*. $n = 4$, each sample pooled of 10 brain–ring gland complexes. (**I**) Epistatic rescue of developmental timing delay in $pvf2^{c0694}$ mutant by overexpression of *pvr* in the prothoracic gland. $n = 3$, 20 larvae per genotype in three independent crosses, 60 larvae in total per condition for (C), (D), and (I). (**J**) Total ecdysone levels in the indicated genotypes, quantified by ELISA at 104 hours AEL. $n = 4$, each sample pooled of 10 larvae of the genotypes indicated for (E) and (J). Data were analyzed by a two-tailed unpaired *t* test, and values represent the means ± SD. $^*P < 0.05$, $^{**}P < 0.01$, $^{***}P < 0.001$, and $^{****}P < 0.0001$.

Nutritional status–dependent *Pvf2* biological activity is regulated by transcription and macrophage numbers

We have shown above that macrophage depletion (*hml*Δ*>rpr*, Fig. 2D) decreases *pvf2* levels, ecdysone synthesis, and delay pupariation. Down-regulation of ras85D in macrophages, which also reduces macrophage numbers by >50% (*61*), has the same effects *pvf2* levels, ecdysone synthesis, and pupariation (fig. S8, A to D). Pvf2 promotes proliferation and survival of macrophages via Pvr in a cell autonomous manner (*50*, *58*, *62*); therefore, regulation of macrophage numbers represents a possible confounding factor for the analysis of the effects of *pvf2* down-regulation. Macrophages are reduced by ~30% in *pvf2* macrophage knockdown larvae (Fig. 4A). Thus, manipulating this axis could alter signal production by macrophages by altering their quantity. However, *pvr* knockdown in hemocytes, which also reduces macrophage numbers by ~30% (Fig. 4A), does not decrease *pvf2* production by macrophages and does not delay pupariation in comparison to controls (Fig. 4B). Macrophage numbers are also reduced by ~30% in starved larvae as well as macrophage *inr*- and *dtor*-knockdown larvae (Fig. 4A). However, reverse transcription quantitative polymerase chain reaction (RT-qPCR) quantification showed a 60 to 80% decrease, of *pvf2* transcripts on a per cell basis, in fluorescence-activated cell sorting (FACS)–sorted macrophages from starved and *inr*-, *dtor*-, and *pvf2*-knockdown larvae (Fig. 4B). Therefore, starvation and *inr*, *dtor*, and *pvf2* knockdown moderately decrease macrophage numbers, which may contribute, in part, to the overall decrease in *pvf2* production, in addition to the transcriptional control of *pvf2* in macrophages.

In addition, we considered the possibility that the production of Pvf2 could be restricted to a subset of macrophages whose survival or proliferation is selectively affected by starvation, deficient InR/dTor, and Pvr signaling. Analysis of *inr*, *dtor*, *pvr*, and *pvf2* expression in a recent *Drosophila* larva single-cell RNA sequencing (RNA-seq) dataset (*63*) showed that *inr*, *dtor*, and *pvr* expression is widely distributed and is not restricted to any potential subset (Fig. 4C). *pvf2* expression itself, although distributed throughout many hemocyte clusters, appears more abundant on a per cell basis in clusters of activated hemocytes (LM1; as well as PM5, PM3, and PM8) in the dataset analyzed in (*63*), consistent with the idea that a threshold of hemocyte activation is associated with *pvf2* transcription. To further investigate whether *pvf2* expression by hemocytes is reduced at the single-hemocyte level under starvation conditions, we used an enhancer-trap transgenic fly that expresses a Gal4 transcription factor under the control of the *pvf2* locus (*64*), to drive expression of green fluorescent protein (GFP) (mcd8::gfp) in Pvf2-expressing cells. Flow cytometry analysis of hemocytes from starved and control *hml*Δ*-dsred;pvf2*$^{tra\text{-}gal4}$*>mcd8::gfp* larvae indicated that ~6% hemocytes express mcd8::gfp in control conditions versus ~2% in starved conditions (Fig. 4D). These results confirm that Pvf2 biological activity is regulated at the transcriptional level under starvation conditions. RNA-seq analysis also indicated that *pvf2*-expressing hemocytes express *hml*, *srp*, and *he* (Fig. 4, D and E), consistent with the biological effects of *pvf2* depletion with the corresponding hemocyte drivers (fig. S4, B and C).

Together, our data indicate that InR and dTor signaling in macrophage licenses ecdysone synthesis via the transcriptional regulation of *pvf2* and, to a lesser extent, by the regulation of hemocyte numbers themselves. These data are consistent with the hypothesis that the expression of *pvf2* by macrophages acts as a developmental checkpoint that licenses Pvr-dependent pupariation if the larval nutritional status, as monitored by InR and dTor, is adequate.

The macrophage *inr/dtor/pvf2* cassette controls the size of adult flies

Delays in critical transitions such as pupariation have systemic effects on organismal and tissue growth (*4*, *17*, *43*, *57*). In particular, delayed pupariation in response to suboptimal food supplies is believed to minimize the effect of nutrient deficiency on the size and fitness of the adult by extending the growth period (*55*). We thus investigated the consequences of the Pvf2/Pvr-dependent developmental delay for the size of pupae and adult *Drosophila*. We found that abrogating the pupariation delay in starved larvae by a *pvf2* transgene further reduced the size of the pupae (Fig. 5A). Conversely, enforcing a Pvr-dependent developmental delay by knockdown or expression of dominant negative forms of *inr*, *dtor*, and *pvf2* in macrophages using several macrophage specific drivers and *pvf2* RNAi lines and in pvf2$^{-/-}$ mutants always resulted in larger pupae under ad libitum feeding condition (Fig. 5, B to D). In addition, the genetic rescue of *pvf2*$^{-/-}$ mutants and the epistatic rescue of *dtor* knockdown larvae by overexpression of a *pvf2* transgene both restored wild-type size (Fig. 5D). In contrast, knockdown of *pvf2* in glia, prothoracic gland, trachea, and fat body had no effect on pupal size (Fig. 5E). Knockdown of *pvf1* and *pvf3* in macrophages had no effect on pupal size either (fig. S7F). Last, the knockdown of *inr*, *dtor*, and *pvf2* in macrophages also generated larger adult flies, both female and male, as measured by wing size (Fig. 5F). To further confirm that the effect of the *inr/dtor/pvf2* cassette on pupal and adult size is mediated by Pvr signaling in the prothoracic gland, we examined the role of *pvr* knockdown, loss of function, or gain of function. Knockdown of *pvr* in the prothoracic gland, but not in macrophages, increased the size of pupae (Fig. 5G). In addition, the pvr hypomorph mutant phenocopied the knockdown of *pvr* in the prothoracic gland (Fig. 5G). Knockdown of *pvr* in the prothoracic gland also increased the sizes of adult female and male flies (Fig. 5H). In contrast, overexpression of *pvr* in the prothoracic gland, which shortens the pupariation time (see Fig. 3G and fig. S6E), decreased the size of pupae (Fig. 5I) and adult flies (Fig. 5H). Last, the size increase observed in null *pvf2*$^{-/-}$ mutants was epistatically rescued by *pvr* overexpression in the prothoracic gland (Fig. 5I). Together, these data demonstrate that control of the Pvr-dependent ecdysone synthesis and pupariation delays by the macrophage *inr/dtor/pvf2* cassette regulates the size of pupae and adult flies from both sexes (Fig. 5J). Of note, pupal and adult size of macrophage-depleted flies was unchanged in comparison from control (fig. S8, E and F), suggesting that macrophage depletion affects other processes that control growth in addition to effects mediated by Pvf2 as also suggested by other studies where macrophage depletion caused reduced (*31*, *65*) or unchanged size (*27*, *45*, *66*).

DISCUSSION

The macrophage *inr/dtor/pvf2* cassette is a developmental timing checkpoint that increases fitness

We report here that validation of the nutritional status of the larvae by the macrophage *inr/dtor/pvf2* genetic cassette is a checkpoint that allows Pvr-dependent ecdysone synthesis in the prothoracic gland and the onset of metamorphosis to proceed. If this nutritional

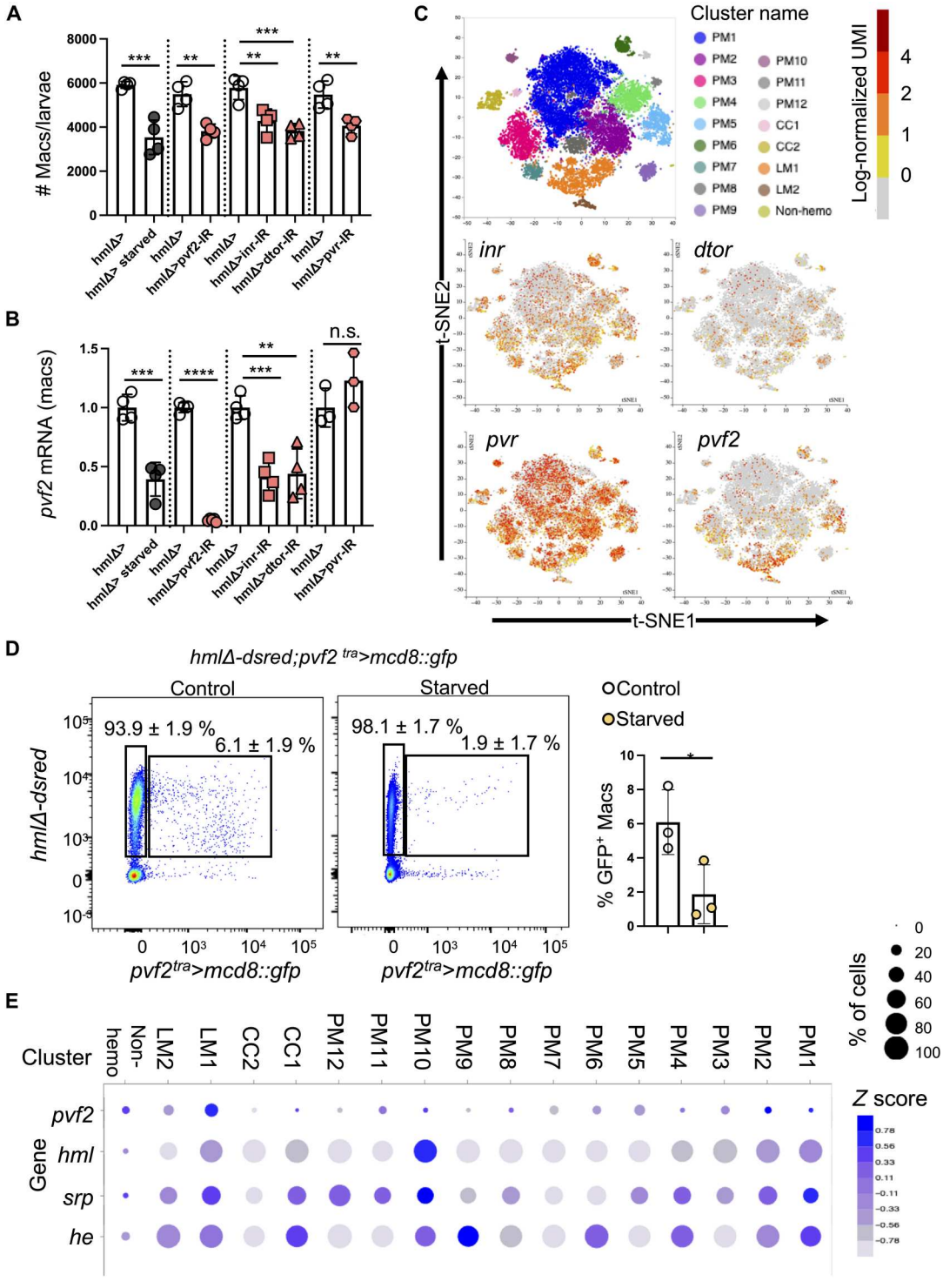

Fig. 4. The macrophage *inr/dtor/pvf2* cassette controls macrophage numbers and *pvf2* expression. (**A**) Quantification of macrophage (Macs) numbers in total larvae at 96 hours AEL by fluorescence-activated cell sorting (FACS)–sorted green fluorescent protein (GFP)$^+$ cells in the indicated genotypes. Dots represent the results from groups of five larvae, $n = 4$ independent experiments. (**B**) Dots represent normalized *pvf2* mRNA levels at 96 hours AEL in 20,000 GFP$^+$ macrophages sorted from 15 to 20 larvae of the indicated genotypes. $n = 3$ to 4 independent experiments. mRNA levels are normalized to *rp49*. (**C**) t-SNE plots from single-cell RNA sequencing (RNA-seq) expression of *inr*, *dtor*, *pvr*, and *pvf2* in wandering larva hemocytes [from (*63*); see Materials and Methods]. (**D**) Flow cytometry and percentage counts of DsRed and GFP-positive macrophages (*hmlΔ-dsred;pvf2^{tra}>mcd8::gfp*) in normal and starved conditions at 96 hours AEL. Numbers in flow cytometry plots represent the percentage of the median and SD cell counts. $n = 3$. (**E**) Dot plot genes to visualize expression changes of *pvf2*, *inr*, *dtor*, *hml*, *srp*, and *he* across different clusters [from (*58*); see Materials and Methods]. Data were analyzed by a two-tailed unpaired *t* test, and values represent the means ± SD. *$P < 0.05$, **$P < 0.01$, ***$P < 0.001$, and ****$P < 0.0001$.

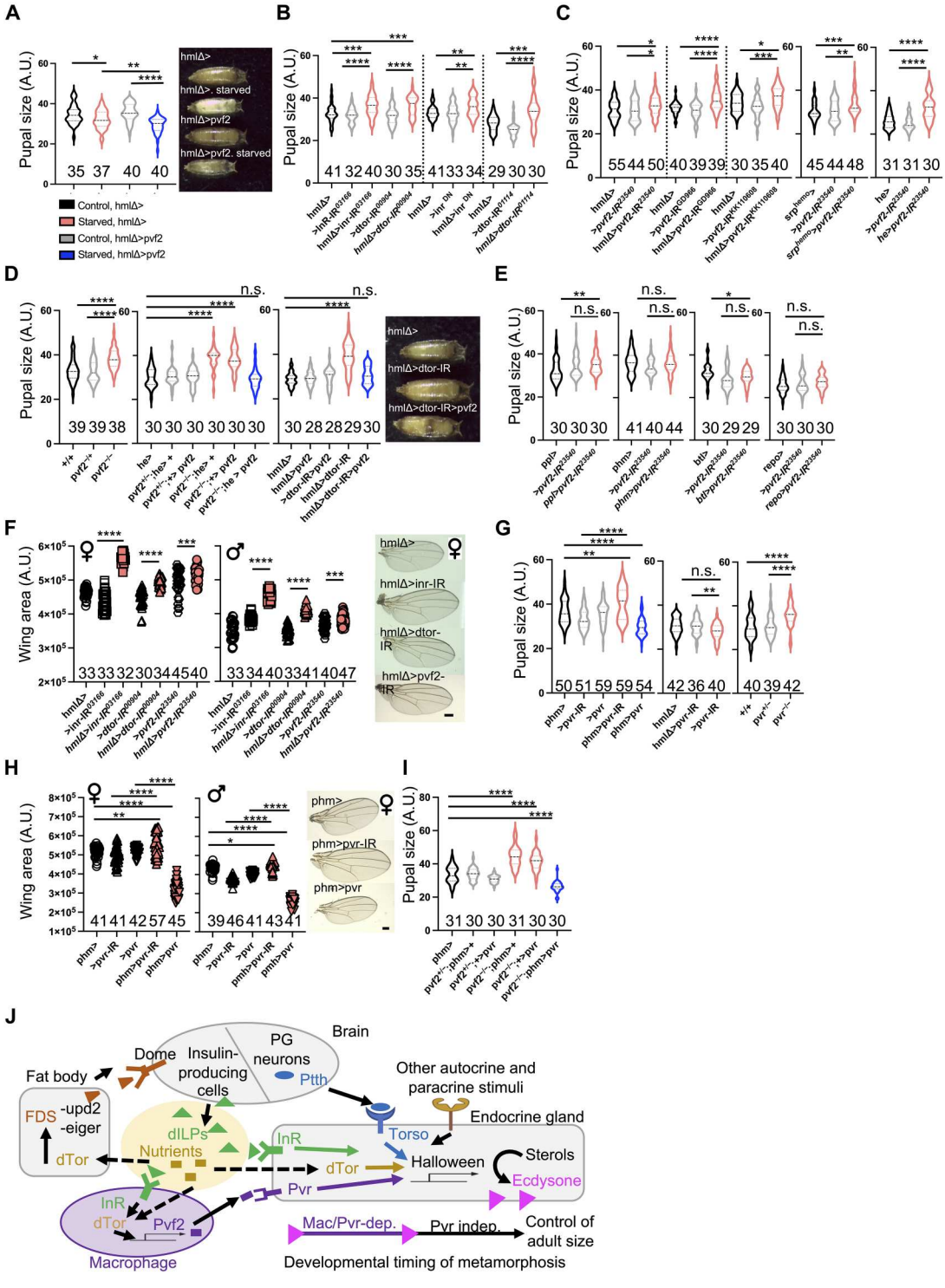

Fig. 5. The macrophage *inr/dtor/pvf2* cassette controls adult size by Pvr in prothoracic gland. (**A**) Final pupal size of starved larvae in the indicated genotypes. (**B**) Final pupal size of *inr* and *dtor* knockdown in macrophages. A.U., arbitrary units. (**C**) Final pupal size of *pvf2* knockdown using different RNAi lines and macrophage drivers. (**D**) Final pupal size in *pvf2*^{c06947} loss-of-function flies, genetic rescue of pupal size in *pvf2*^{c0694} loss-of-function mutant by overexpression of pvf2, and epistatic rescue of pupal size in *dtor*-lacking macrophages mutant by overexpression of *pvf2*. (**E**) Final pupal size upon *pvf2* knockdown in fat body (*ppl-gal4*), prothoracic gland (*phm-gal4*), trachea (*btl-gal4*), and glia cells (*repo-gal4*). (**F**) Wing area of female and male virgin flies of *inr*, *dtor*, and *pvf2* knockdown in macrophage. (**G**) Final pupal size upon *pvr* knockdown or *pvr* overexpression in prothoracic gland, knockdown of *pvr* in macrophages, and in *pvr*^{01} hypomorph mutant. (**H**) Wing area of female and male virgin flies upon *pvr* knockdown or *pvr* overexpression in prothoracic gland. (**I**) Epistatic rescue of pupal size in *pvf2*^{c0694} loss-of-function mutant by overexpression of *pvr* in prothoracic gland. Numbers along the *x* axis of the graphs indicate the number of flies analyzed. Data were analyzed by a two-tailed unpaired *t* test, and values represent the means ± SD. *P < 0.05, **P < 0.01, ***P < 0.001, and ****P < 0.0001. (**J**) Working model for the role of the *inr/dtor/pvf2* cassette in macrophages (purple colors) as a nutritional status checkpoint in the context of current knowledge of the timing of metamorphosis by the brain, the fat body, nutritional status, and steroid hormone biosynthesis in the prothoracic gland. Purple arrow indicates the control of a Pvr-dependent stage of ecdysone biosynthesis under the control of macrophages. FDS, fat-body-derived signals.

status is not met, here in the case of a starvation event, low Pvf2 production delays ecdysone synthesis and opens a time window of an extra ~8 hours for preparing pupariation, after which Pvr-independent ecdysone synthesis and pupariation occur (Fig. 5J). The physiological significance of this time window controlled by macrophages and Pvr expression in the prothoracic gland for the fitness of the host is best illustrated by its consequence on the fitness, here the size, of pupae and adult flies, as opening the window allows the formation of larger flies and can rescue the effect of a starvation episode at the larval stage (*42*, *55*).

These findings support and extend the general concept that macrophages can act as metabolic sensors that integrate environmental

signals to contribute to organismal homeostasis (*22*, *26*). More precisely, the results from this study shows that macrophages represent a step in a complex and highly regulated interorgan communication process that allows for fine-tuning of developmental timing. The role of macrophages appears to be to delay the timing of the developmental program when the nutritional status of the larvae is poor, as assessed by InR/dTor signaling, but early/increased *pvf2* expression does not initiate premature Pvr-mediated pupariation. In contrast, the timing of Pvr-mediated pupariation is determined by expression of Pvr in the prothoracic gland, which is up-regulated just before the onset of normal pupariation, while *pvr* early/overexpression induces early pupariation and strongly decreases the size of the adult flies. Moreover, in the absence of Pvf2 or Pvr, pupariation will eventually proceed, in a Pvr-independent manner, at the cost of a reduced size of the flies.

Macrophages assess nutritional status via InR/Tor signaling

Our results suggest that macrophages sense the nutritional status of the larvae via insulin/TOR signaling. This is consistent with seminal studies that have shown that the insulin/TOR signaling network transduces nutritional signals that regulate cell growth and developmental timing at the organismal level (*14*, *17*, *67*, *68*). DILP synthesis and secretion by insulin-producing cells, like insulin in mammals (*51*, *69*), are stimulated directly and indirectly by fat body–secreted factors such as Unpaired 2, Eiger, and Stunted that are decreased in starvation conditions (Fig. 5J) (*70*–*73*). DILPs circulate in the hemolymph and are thus available to macrophages. In addition, dTor, as well as the mammalian TOR complex, is activated by InR signaling and also directly by nutrients, specifically amino acids (*52*). The InR also signals independently of Tor by inhibiting Foxo (*51*), but our results indicate that FOXO overexpression does not affect the timing of pupariation (see fig. S7D), while dTOR is both necessary and sufficient for Pvf2 production by macrophages and for pupariation. We did not observe an effect of the knockdown of individual nuclear receptors in macrophages (see fig. S3), suggesting that they do not regulate Pvf2 production. Therefore, it is likely that insulin/TOR signaling in hemocytes is activated, at least, in part, by the availability of DILPs and amino acids; nevertheless, it is very possible that macrophages integrate additional yet unidentified signals to control *pvf2* transcription and steroid hormone biosynthesis. On the other hand, InR/TOR signaling in the prothoracic gland itself also controls the timing of metamorphosis (*17*, *42*, *68*), indicating that this critical pathway collects and integrates information from different tissues to regulate developmental timing at the organismal level.

Bioavailability of *Pvfs* in the prothoracic gland

Drosophila Pvr has three ligands coded by separate genes—*pvf1*, *pvf2* and *pvf3*—with partially redundant functions in cell survival, migration, and proliferation during embryonical stages (*50*, *58*, *74*, *75*). Our results suggest that Pvf2, but not Pvf1 and Pvf3, is required to activate Pvr in the prothoracic gland to regulate ecdysone synthesis and developmental timing under physiological conditions. Among possible explanations, we show here that *pvf2* expression is 10- to 100-fold higher in larval macrophages as compared to *pvf1* and *pvf3* (fig. S2C). In addition, there are 13 isoforms of Pvr (https://flybase.org/); therefore, it is possible that the prothoracic gland expresses Pvr(s) isoform(s) with extracellular ligand binding domain specific for Pvf2. It is also possible that larval macrophages that produce Pvf2 are in close contact with the prothoracic gland or that Pvf2 produced by hemocytes circulates in hemolymph and thus accesses the prothoracic gland more readily than Pvfs produced by other tissues. In addition, we cannot eliminate the possibility of unknown biochemical differences between Pvfs that could affect, for example, their solubility in the hemolymph, of the existence of putative coreceptor(s). Last, although Pvf2 is required, the contribution of the other Pvfs cannot be ruled out. It was shown that Pvr can regulate ecdysone synthesis in the prothoracic gland in an autocrine manner via Pvf2 and Pvf3, which are both expressed in the prothoracic gland at late stages during development (*57*), and a local source of Pvf3 may thus contribute to early pupariation of *pvf2* mutant overexpressing *pvr*.

Macrophages license steroid hormone biosynthesis in the endocrine gland

Steroid hormone production in the endocrine gland of the fly and metamorphosis are under the control of the GnRH superfamily hormone Crz and Asta/AstaR via the PTTH produced by the PTTH neurons (*4*, *7*, *11*–*13*). A notable finding from our study is that the production of Pvf2 by macrophages contributes orthogonally to steroidogenesis by promoting transcription of the Halloween steroid biosynthesis genes when a satisfactory nutritional status is detected (see Fig. 5J). The development and organismal homeostasis of *Drosophila* and mammals are highly conserved (*76*), and the production of steroid hormones in mammalian puberty is under the control of the hypothalamus GnRH via the anterior pituitary hormones LH and FSH (*2*, *3*, *6*), which are similar to the Crz-Ptth axis (*13*) although LH and FSH are not Ptth orthologs. Although an orthogonal role of macrophages in the regulation of puberty is yet unknown, it is well documented that macrophage-deficient mice present with steroid hormone deficiency and infertility (*77*–*84*), and several mouse Pvfs orthologs (PDGFs) are also important for steroid production and male and female fertility (*85*).

MATERIALS AND METHODS

Drosophila husbandry

Plasmatocyte-specific reporter line and driver hmlΔ-gal4;UAS-2xeGFP stock is a gift from S. Sinenko (*86*). UAS-pvf2 is a gift from B. Lemaitre (*61*). srp^{hemo}-gal4 is a gift from N. Perrimon. ras85D- KK108029-IR is a gift from M. Dominguez. $pvf2^{tra\text{-}gal4}$ is a gift from T. K. Johnson. hmlΔ-dsred (III). spi-TRiP.HMS01120-RNAi, gbb-TRiP.HMS01243-RNAi, dpp-TRiP.JF01090-RNAi, pvf1-TRiP.HMS01958-RNAi, pvf2-TRiP.HMJ23540-RNAi, pvf3-TRiP.HMS01876-RNAi, dilp6-TRiP.HMS00549-RNAi, spz-TRiP.HM05024-RNAi, upd2-TRiP.HMS00948-RNAi, upd3-TRiP.HM05061-RNAi, akh-TRiP.HMS00477-RNAi, idgf2-TRiP.HMC04223-RNAi, idgf6-TRiP.HMC04127-RNAi, pvr-TRiP.HMS01662-RNAi, hr96-TRiP.JF02350, eip78c-TRiP.JF02258, eip75b-TRiP.HMS01530, hr39-TRiP.JF02432, hr3-TRiP.HMC03156, hnf4-TRiP.JF02539, usp-TRiP.HMS01620, hr78-TRiP.JF03424, ecr-TRiP.HMJ22371, err-TRiP.HMC03087, hr4-TRiP.HM05260, svp-TRiP.JF03105, inr-TRiP.HMS03166, elav-gal4, btl-gal4, phm-gal4, ppl-gal4, repo-gal4, he-gal4, UAS-reaper, UAS-inrDN, dtor-TRiP.HMS00904, dtor-TRiP.HMS01114, UAS-pvr, Pvf2c06947, Pvr1, UAS-pvf1.RB, and pvf2d02444 lines are from the Bloomington Stock Center at Indiana University (Bloomington, IN). pvf1-KK112211-RNAi,

pvf1-GD3432-RNAi, pvf2-KK110608-RNAi, pvf2-GD966-RNAi, pvf3-KK112796-RNAi, and pvf3-GD5238-RNAi are from Vienna *Drosophila* Resource Center. Flies were reared in standard molasses fly food from Archon scientific at 25°C (except when indicated) on a 12-hour:12-hour light:dark cycle.

Targeted RNAi screen for genes encoding secreted factors and nutrient-sensing receptors in larval macrophages

Genes involve in tissue growth and developmental timing were obtained from RNA-seq analysis of embryonic macrophages from (*49*). The expression of genes in larvae macrophages was determined by RT-qPCR of sorted macrophages at 96 hours AEL, and their role in developmental timing was tested using RNAi lines from Bloomington Stock Center at Indiana University (Bloomington, IN) listed above and the hmlΔ-gal4;UAS-2xeGFP flies.

Egg-laying and pupariation formation measurements

We crossed 20 females and males, and, after 48 hours, the parental flies were transferred to grape agar plates (Nutri-fly grape agar premix from Genesee Scientific) with yeast paste and left 3 to 4 hours for egg deposition at 25°C. The flies were removed, and laid eggs were incubated 48 hours at 25°C. Forty-eight hours later, the second-instar larvae were transferred onto *Drosophila* molasses food (20 larvae per tube) and reared at 26.5°C. We check the transition between larva-to-pupa at 8-hour intervals, with "time 0" designated as 4 hours after the initiation of egg laying and referred to as "AEL." Median time of pupariation was used to analyze differences between genotypes (50% of larvae that became pupae).

Critical weight and starvation experiments

To determine the length of the pre-CW phase, we transferred the larva at 48 hours AEL into petri dishes with *Drosophila* molasses food (20 larvae per dish), and we allowed the larva to develop. At the different time points indicated (72, 76, 80, 84, 88, 92, and 96 hours AEL; fig S1A), we transferred the larva to empty petri dishes with a wet paper in the cover to keep larvae hydrated and avoid desiccation to starve the larvae until they enter in pupariation (*87*). We counted pupariation formation in 4-hour intervals.

On the basis of these results, all starvation experiments were performed by transferring 88 hours AEL pre-CW larvae to empty petri dishes with a wet paper in the cover to keep larvae hydrated and avoid desiccation (*87*). After 8 hours, the larvae were refed by transferring then to *Drosophila* molasses food tubes with 5 ml, and we counted pupariation formation in 8-hour intervals.

Pupae volume measurements

Twenty females and 20 males were crossed and left 24 hours for egg deposition. Parental flies were transferred every 24 hours to fresh tubes, and laid eggs were reared at 25°C. Pupae were collected and photographed with their dorsal side up. Length and width were measured using ImageJ; volume was calculated according to the following formula: $v = 4/3\pi(L/2)(l/2)2$ (L, length; and l, width) (*88*). Leica M80 stereo microscope was used for pupal imagine.

Adult wing area measurements

Twenty females and 20 males were crossed and left 24 hours for egg deposition. Parental flies were transferred every 24 hours to fresh tubes, and laid eggs were reared at 25°C. Adults were collected, and left wings of each individual were excised and rinsed thoroughly with ethanol and mounted in a glycerol-ethanol solution. Wing areas were measured using ImageJ (*89*). Pictures were taken using an Axio Lab.A1 Zeiss microscope with N-Achroplan 5×/01.25 objective.

Whole-larva mounting and confocal imaging

Mild-late L3 larvae were rinsed with tap water (no longer than 5 min), dried carefully, and anaesthetized using diethyl ether for less than 3.5 min. Larvae were positioning within one cover slide and a slide for mounting immobilizing the sample and imagine. We set up the tile scan with the micrometer-thick Z stack on LSM880 Zeiss microscope with 5× objective, which allows to see the sessile macrophages in the cuticle. Images were acquired with a resolution of 1024 × 1024.

Immunohistochemistry in ring-gland tissue

Brain–ring gland complex was dissected out in cold phosphate-buffered saline (PBS) buffer and fixed in 4% paraformaldehyde for 20 min (*90*). Brain–ring gland complex was stained overnight at 4°C with chicken anti-GFP (1/500; Life Technologies), and rat anti-Pvr (*91*) (1/500; a gift from B. Shilo). Secondary antibodies 488 anti-chicken (1/500) and 647 anti-rat (1/500) were purchased from Invitrogen. For DNA and nuclei staining, we used Hoechst (1/1000) for 10 min at room temperature. We set up the tile scan with the micrometer-thick Z stack on an LSM880 Zeiss microscope with 40× oil objective. Images were acquired with a resolution of 1024 × 1024.

Flow cytometry analysis of macrophages

Macrophages counts

Hemocytes from five larvae at 96 hours AEL were bled into 120 μl of FACS buffer (PBS, 0.5% bovine serum albumin, and 2 mM EDTA) containing 1 nM phenylthiourea (Sigma-Aldrich, St. Louis, MO, USA) to prevent melanization. We used two forceps to make an incision from the posterior and pull to the anterior ends of the larvae. We allow larvae to bleed for a few seconds, and, later, we carefully scrape the lateral cuticle to avoid the lymph gland disruption (*61*). We counted the macrophage numbers by sorted live GFP-positive hemocytes [4′,6-diamidino-2-phenylindole (DAPI) negative], using hmlΔ>eGFP, in on an BD FACSARIA III (BD Biosciences). Flow cytometry plots were obtained with FlowJo 9.9.

Pvf2 transcriptional reporter

Hemocytes from 10 to 15 hmlΔ-dsred;pvf2^{tra}>mcd8::gfp larvae at 96 hours AEL in fed condition and starved condition (8 hours starved from 88 hours AEL) were bled and analyzed as above. Percentage (%) of live DsRed positive and GFP-positive hemocytes (DAPI negative), using in on an ARIA III (BD Biosciences), was determined by flow cytometry using Flow Jo 9.9 as above.

May-Grunwald–Giemsa staining

Analysis of macrophages was done on of sorted cells from GFP-positive hemocytes population, using HmlΔ>eGFP. One thousand cells were sorted directly in fetal bovine serum (Invitrogen) and centrifuged for 10 min at 800*g* with a low acceleration onto Superfrost slides (Thermo Fisher Scientific). After air drying for at least 30 min, the slides were fixed in methanol, air dried for at least 30 min, stained with May-Grunwald (Sigma-Aldrich) solution for 5

to 15 min and then Giemsa (Sigma-Aldrich) solution 14% for 15 to 30 min, and rinsed with Sorenson buffer (pH 6.8). After air drying, the slides were mounted with Entellan (Merck). Pictures were taken using an Axio Lab.A1 Zeiss microscope with N-Achroplan 100×/01.25 objective.

qRT-PCR on sorted macrophages and whole larvae

For qRT-PCR, 20,000 hemocytes were sorted into 600 µl of TRIzol LS (Life Technologies). RNA extraction was performed following the manufacturer′s instructions (miRNeasy Mini Kit, Qiagen). RNA concentration was measured with NanoDrop 2000. cDNA preparation was performed with the Invitrogen SuperScript IV First-Strand Synthesis System (Thermo Fisher Scientific) as per the manufacturer′s instructions. qRT-PCR was done with 5 to 10 ng of cDNA. For whole larvae, qRT-PCR tissue homogenization was performed with a tissue lyser (Precellys Evolution, Bertin Technologies) in 2 ml of tissue-homogenizing mixed beads (Bertin Technologies, ref. P000918-LYSK0-A) of five larvae per sample, and RNA extraction was performed following the manufacturer′s instructions (RNeasy Mini Kit, Qiagen). For whole larva, the same protocol as for the sorted cells and the qRT-PCR was performed on 500 ng of cDNA. qRT-PCR was performed using QuantStudio 6 Flex Real-Time PCR from Life Technologies. qRT-PCR is performed on a QuantStudio 6 Flex using TaqMan Fast Advance Mastermix and TaqMan probes for rp49 (Dm02151827_g1), dib (Dm01843083_g1), phm (Dm01844265_g1), nvd (Dm03419116_m1), sad (Dm02139323_g1), spo (Dm01840221_s1), eip75b (Dm01793666_m1), idgf2 (Dm01842858_g1), idgf6 (Dm01842553_g1), gbb (Dm01843010_s1), dpp (Dm01842959_m1), akh (Dm01822073_g1), spi (Dm02364865_s1), spz (Dm02151534_g1), spz2 (Dm01832735_g1), spz3 (Dm01809417_m1), spz4 (Dm01810735_g1), spz5 (Dm01835260_m1), spz6 (Dm01834239_g1), dilp6 (Dm01829746_g1), upd2 (Dm01844134_g1), upd3 (Dm01844142_g1), pvf2 (Dm01814370_m1), pvf1 (Dm01814376_m1), pvf3 (Dm01813949_m1), pvr (Dm01803625_m1), hr96 (Dm02151377_m1), eip78c (Dm01798025_g1), hr39 (Dm01811265_g1), hr3 (Dm01846760_m1), hnf4 (Dm01803764_g1), usp (Dm01841709_s1), hr78 (Dm01798077_g1), ecr (Dm01811604_g1), err (Dm01835887_g1), hr4 (Dm01798975_g1), hr38 (Dm01842602_g1), hr83 (Dm02137429_g1), hr51 (Dm01824332_m1), svp (Dm02135706_m1), dsf (Dm01842632_m1), tll (Dm02151861_g1), inr (Dm02136218_g1), dtor (Dm01843300_g1), and 4e-bp (Dm01842928_g1).

Ecdysteroid measurement

For ecdysteroid extraction, 10 whole larvae from each condition (from 96 or 104 hours AEL, as indicate in the figure) were collected in 2 ml of tissue-homogenizing mixed beads (Bertin Technologies, ref. P000918-LYSK0-A) and frozen in liquid nitrogen and transfer to −80°C. Samples were homogenized using a tissue lyser (Precellys Evolution, Bertin Technologies) in 0.3 ml of methanol, centrifuged at maximum speed for 5 min at room temperature and the supernatant was transferred to another eppendorf tube. We repeat this procedure by adding 0.3 ml of methanol to the pellet and mix using vortex and a third round using 0.3 ml of ethanol. The pooled sample after homogenization was 0.9 ml per sample. For quantification, the extracted samples were centrifuged at maximum speed for 5 min (room temperature) to remove any remaining debris and divided into two tubes to generate technical replicates. The cleared samples were evaporated overnight (*92*). The following steps were performed using the 20-HE enzyme-linked immunosorbent assay kit instructions (Bertin Pharma, no. A05120; 96 wells). Absorbance was measured at 410 nm with a microplate reader (SpectraMax i3 from Molecular devices).

20-HE treatment

Larvae were collected as explain above and transferred onto *Drosophila* molasses at 48 hours AEL. Control larvae (*hml*Δ*>gfp*) and mutant conditions (*hml*Δ*>pvf2-IR* and *hml*Δ*>rpr*) were transferred at 80 hours AEL to fresh food supplemented with 20-HE (0.5 mg/ml; Sigma-Aldrich, H5142) diluted in ethanol. We used ethanol as a control vehicle.

Single-cell gene expression visualization by dot plots

Dot plots were generated using a user-friendly searchable web tool (www.flyrnai.org/scRNA/blood/) where genes can be queried and visualized in the different clusters made by single-cell RNA-seq (*63*).

Statistical analyses

All statistical analyses were performed using GraphPad Prism Software 9.0 with a 95% confidence limit ($P < 0.05$). An unpaired t test was used for comparisons between two genotypes or time points.

Animal experiments

All animal experiments were done using *D. melanogaster*, and it is not subject of ethics committee.

Supplementary Materials

This PDF file includes:

Figs. S1 to S8

REFERENCES AND NOTES

1. R. S. Poethig, Phase change and the regulation of developmental timing in plants. *Science* **301**, 334–336 (2003).
2. T. M. Plant, Neuroendocrine control of the onset of puberty. *Front. Neuroendocrinol.* **38**, 73–88 (2015).
3. B. Bordini, R. L. Rosenfield, Normal pubertal development: Part I: The endocrine basis of puberty. *Pediatr. Rev.* **32**, 223–229 (2011).
4. Z. McBrayer, H. Ono, M. Shimell, J. P. Parvy, R. B. Beckstead, J. T. Warren, C. S. Thummel, C. Dauphin-Villemant, L. I. Gilbert, M. B. O'Connor, Prothoracicotropic hormone regulates developmental timing and body size in *Drosophila*. *Dev. Cell* **13**, 857–871 (2007).
5. K. F. Rewitz, N. Yamanaka, L. I. Gilbert, M. B. O'Connor, The insect neuropeptide PTTH activates receptor tyrosine kinase torso to initiate metamorphosis. *Science* **326**, 1403–1405 (2009).
6. A. E. Herbison, Control of puberty onset and fertility by gonadotropin-releasing hormone neurons. *Nat. Rev. Endocrinol.* **12**, 452–466 (2016).
7. D. Deveci, F. A. Martin, P. Leopold, N. M. Romero, AstA signaling functions as an evolutionary conserved mechanism timing juvenile to adult transition. *Curr. Biol.* **29**, 813–822.e4 (2019).
8. D. M. Vallejo, S. Juarez-Carreno, J. Bolivar, J. Morante, M. Dominguez, A brain circuit that synchronizes growth and maturation revealed through Dilp8 binding to Lgr3. *Science* **350**, aac6767 (2015).
9. A. Garelli, F. Heredia, A. P. Casimiro, A. Macedo, C. Nunes, M. Garcez, A. R. M. Dias, Y. A. Volonte, T. Uhlmann, E. Caparros, T. Koyama, A. M. Gontijo, Dilp8 requires the neuronal relaxin receptor Lgr3 to couple growth to developmental timing. *Nat. Commun.* **6**, 8732 (2015).

10. J. Colombani, D. S. Andersen, L. Boulan, E. Boone, N. Romero, V. Virolle, M. Texada, P. Leopold, Drosophila Lgr3 couples organ growth with maturation and ensures developmental stability. *Curr. Biol.* **25**, 2723–2729 (2015).
11. N. Yamanaka, K. F. Rewitz, M. B. O'Connor, Ecdysone control of developmental transitions: Lessons from *Drosophila* research. *Annu. Rev. Entomol.* **58**, 497–516 (2013).
12. K. F. Rewitz, N. Yamanaka, M. B. O'Connor, Developmental checkpoints and feedback circuits time insect maturation. *Curr. Top. Dev. Biol.* **103**, 1–33 (2013).
13. E. Imura, Y. Shimada-Niwa, T. Nishimura, S. Huckesfeld, P. Schlegel, Y. Ohhara, S. Kondo, H. Tanimoto, A. Cardona, M. J. Pankratz, R. Niwa, The corazonin-PTTH neuronal axis controls systemic body growth by regulating basal ecdysteroid biosynthesis in *Drosophila melanogaster*. *Curr. Biol.* **30**, 2156–2165.e5 (2020).
14. J. M. Bateman, H. McNeill, Temporal control of differentiation by the insulin receptor/tor pathway in *Drosophila*. *Cell* **119**, 87–96 (2004).
15. E. Villamor, E. C. Jansen, Nutritional determinants of the timing of puberty. *Annu. Rev. Public Health* **37**, 33–46 (2016).
16. E. T. Danielsen, M. E. Moeller, K. F. Rewitz, Nutrient signaling and developmental timing of maturation. *Curr. Top. Dev. Biol.* **105**, 37–67 (2013).
17. S. Layalle, N. Arquier, P. Leopold, The TOR pathway couples nutrition and developmental timing in *Drosophila*. *Dev. Cell* **15**, 568–577 (2008).
18. J. M. Tanner, Trend towards earlier menarche in London, Olso, Copenhagen, the Netherlands and Hungary. *Nature* **243**, 95–96 (1973).
19. L. Zacharias, R. J. Wurtman, Age at menarche. Genetic and environmentalinfluences. *N. Engl. J. Med.* **280**, 868–875 (1969).
20. J. C. Marshall, R. P. Kelch, Low dose pulsatile gonadotropin-releasing hormone in anorexia nervosa: A model of human pubertal development. *J. Clin. Endocrinol. Metab.* **49**, 712–718 (1979).
21. S. Juarez-Carreno, D. M. Vallejo, J. Carranza-Valencia, M. Palomino-Schatzlein, P. Ramon-Canellas, R. Santoro, E. de Hartog, D. Ferres-Marco, A. Romero, H. P. Peterson, E. Ballesta-Illan, A. Pineda-Lucena, M. Dominguez, J. Morante, Body-fat sensor triggers ribosome maturation in the steroidogenic gland to initiate sexual maturation in *Drosophila*. *Cell Rep.* **37**, 109830 (2021).
22. Y. Okabe, R. Medzhitov, Tissue biology perspective on macrophages. *Nat. Immunol.* **17**, 9–17 (2016).
23. K. S. Gold, K. Bruckner, Macrophages and cellular immunity in *Drosophila melanogaster*. *Semin. Immunol.* **27**, 357–368 (2015).
24. W. Wood, P. Martin, Macrophage functions in tissue patterning and disease: New insights from the fly. *Dev. Cell* **40**, 221–233 (2017).
25. L. C. Rankin, D. Artis, Beyond host defense: Emerging functions of the immune system in regulating complex tissue physiology. *Cell* **173**, 554–567 (2018).
26. N. Cox, M. Pokrovskii, R. Vicario, F. Geissmann, Origins, biology, and diseases of tissue macrophages. *Annu. Rev. Immunol.* **39**, 313–344 (2021).
27. N. Cox, L. Crozet, I. R. Holtman, P. L. Loyher, T. Lazarov, J. B. White, E. Mass, E. R. Stanley, O. Elemento, C. K. Glass, F. Geissmann, Diet-regulated production of PDGFcc by macrophages controls energy storage. *Science* **373**, eabe9383 (2021).
28. K. J. Woodcock, K. Kierdorf, C. A. Pouchelon, V. Vivancos, M. S. Dionne, F. Geissmann, Macrophage-derived upd3 cytokine causes impaired glucose homeostasis and reduced lifespan in *Drosophila* fed a lipid-rich diet. *Immunity* **42**, 133–144 (2015).
29. T. T. Chen, T. A. Lane, M. C. Doody, M. R. Caudle, The effect of peritoneal macrophage-derived factor(s) on ovarian progesterone secretion and LH receptors: The role of calcium. *Am. J. Reprod. Immunol.* **28**, 43–50 (1992).
30. X. W. Gu, S. Y. Li, S. Matsuyama, T. DeFalco, Immune cells as critical regulators of steroidogenesis in the testis and beyond. *Front. Endocrinol.* **13**, 894437 (2022).
31. M. Shin, N. Cha, F. Koranteng, B. Cho, J. Shim, Subpopulation of macrophage-like plasmatocytes attenuates systemic growth via JAK/STAT in the *Drosophila* fat body. *Front. Immunol.* **11**, 63 (2020).
32. C. E. Jacome-Galarza, G. I. Percin, J. T. Muller, E. Mass, T. Lazarov, J. Eitler, M. Rauner, V. K. Yadav, L. Crozet, M. Bohm, P. L. Loyher, G. Karsenty, C. Waskow, F. Geissmann, Developmental origin, functional maintenance and genetic rescue of osteoclasts. *Nature* **568**, 541–545 (2019).
33. P. E. Cohen, K. Nishimura, L. Zhu, J. W. Pollard, Macrophages: Important accessory cells for reproductive function. *J. Leukoc. Biol.* **66**, 765–772 (1999).
34. E. Lokka, L. Lintukorpi, S. Cisneros-Montalvo, J. A. Makela, S. Tyystjarvi, V. Ojasalo, H. Gerke, J. Toppari, P. Rantakari, M. Salmi, Generation, localization and functions of macrophages during the development of testis. *Nat. Commun.* **11**, 4375 (2020).
35. R. J. Norman, M. Brannstrom, White cells and the ovary–Incidental invaders or essential effectors? *J. Endocrinol.* **140**, 333–336 (1994).
36. Z. Zhang, L. Huang, L. Brayboy, Macrophages: An indispensable piece of ovarian health. *Biol. Reprod.* **104**, 527–538 (2021).
37. P. E. Cohen, L. Zhu, K. Nishimura, J. W. Pollard, Colony-stimulating factor 1 regulation of neuroendocrine pathways that control gonadal function in mice. *Endocrinology* **143**, 1413–1422 (2002).
38. P. E. Cohen, M. P. Hardy, J. W. Pollard, Colony-stimulating factor-1 plays a major role in the development of reproductive function in male mice. *Mol. Endocrinol.* **11**, 1636–1650 (1997).
39. P. E. Cohen, O. Chisholm, R. J. Arceci, E. R. Stanley, J. W. Pollard, Absence of colony-stimulating factor-1 in osteopetrotic (csfmop/csfmop) mice results in male fertility defects. *Biol. Reprod.* **55**, 310–317 (1996).
40. J. B. Yee, J. C. Hutson, Effects of testicular macrophage-conditioned medium on Leydig cells in culture. *Endocrinology* **116**, 2682–2684 (1985).
41. M. M. Matzuk, D. J. Lamb, The biology of infertility: Research advances and clinical challenges. *Nat. Med.* **14**, 1197–1213 (2008).
42. Y. Ohhara, S. Kobayashi, N. Yamanaka, Nutrient-dependent endocycling in steroidogenic tissue dictates timing of metamorphosis in *Drosophila melanogaster*. *PLOS Genet.* **13**, e1006583 (2017).
43. T. Koyama, M. A. Rodrigues, A. Athanasiadis, A. W. Shingleton, C. K. Mirth, Nutritional control of body size through FoxO-Ultraspiracle mediated ecdysone biosynthesis. *eLife* **3**, e03091 (2014).
44. W. A. Segraves, D. S. Hogness, The E75 ecdysone-inducible gene responsible for the 75B early puff in *Drosophila* encodes two new members of the steroid receptor superfamily. *Genes Dev.* **4**, 204–219 (1990).
45. B. Charroux, J. Royet, Elimination of plasmatocytes by targeted apoptosis reveals their role in multiple aspects of the *Drosophila* immune response. *Proc. Natl. Acad. Sci. U.S.A.* **106**, 9797–9802 (2009).
46. H. N. Stephenson, R. Streeck, F. Grublinger, C. Goosmann, A. Herzig, Hemocytes are essential for *Drosophila melanogaster* post-embryonic development, independent of control of the microbiota. *Development* **149**, dev200286 (2022).
47. L. I. Gilbert, R. Rybczynski, J. T. Warren, Control and biochemical nature of the ecdysteroidogenic pathway. *Annu. Rev. Entomol.* **47**, 883–916 (2002).
48. A. Mase, J. Augsburger, K. Bruckner, Macrophages and their organ locations shape each other in development and homeostasis – A *Drosophila* perspective. *Front. Cell Dev. Biol.* **9**, 630272 (2021).
49. V. Belyaeva, S. Wachner, A. Gyoergy, S. Emtenani, I. Gridchyn, M. Akhmanova, M. Linder, M. Roblek, M. Sibilia, D. Siekhaus, Fos regulates macrophage infiltration against surrounding tissue resistance by a cortical actin-based mechanism in *Drosophila*. *PLOS Biol.* **20**, e3001494 (2022).
50. N. K. Cho, L. Keyes, E. Johnson, J. Heller, L. Ryner, F. Karim, M. A. Krasnow, Developmental control of blood cell migration by the *Drosophila* VEGF pathway. *Cell* **108**, 865–876 (2002).
51. J. Boucher, A. Kleinridders, C. R. Kahn, Insulin receptor signaling in normal and insulin-resistant states. *Cold Spring Harb. Perspect. Biol.* **6**, a009191 (2014).
52. R. A. Saxton, D. M. Sabatini, mTOR signaling in growth, metabolism, and disease. *Cell* **169**, 361–371 (2017).
53. A. R. Saltiel, C. R. Kahn, Insulin signalling and the regulation of glucose and lipid metabolism. *Nature* **414**, 799–806 (2001).
54. J. S. Britton, W. K. Lockwood, L. Li, S. M. Cohen, B. A. Edgar, *Drosophila's* insulin/PI3-kinase pathway coordinates cellular metabolism with nutritional conditions. *Dev. Cell* **2**, 239–249 (2002).
55. A. W. Shingleton, J. Das, L. Vinicius, D. L. Stern, The temporal requirements for insulin signaling during development in *Drosophila*. *PLoS Biol.* **3**, e289 (2005).
56. S. S. Grewal, Insulin/TOR signaling in growth and homeostasis: A view from the fly world. *Int. J. Biochem. Cell Biol.* **41**, 1006–1010 (2009).
57. X. Pan, M. B. O'Connor, Coordination among multiple receptor tyrosine kinase signals controls *Drosophila* developmental timing and body size. *Cell Rep.* **36**, 109644 (2021).
58. K. Bruckner, L. Kockel, P. Duchek, C. M. Luque, P. Rorth, N. Perrimon, The PDGF/VEGF receptor controls blood cell survival in *Drosophila*. *Dev. Cell* **7**, 73–84 (2004).
59. H. Zheng, X. Wang, P. Guo, W. Ge, Q. Yan, W. Gao, Y. Xi, X. Yang, Premature remodeling of fat body and fat mobilization triggered by platelet-derived growth factor/VEGF receptor in *Drosophila*. *FASEB J.* **31**, 1964–1975 (2017).
60. R. D. Read, Pvr receptor tyrosine kinase signaling promotes post-embryonic morphogenesis and survival of glia and neural progenitor cells in *Drosophila*. *Development* **145**, dev164285 (2018).
61. E. Ramond, B. Petrignani, J. P. Dudzic, J. P. Boquete, M. Poidevin, S. Kondo, B. Lemaitre, The adipokine NimrodB5 regulates peripheral hematopoiesis in *Drosophila*. *FEBS J.* **287**, 3399–3426 (2020).
62. A. I. Munier, D. Doucet, E. Perrodou, D. Zachary, M. Meister, J. A. Hoffmann, C. A. Janeway Jr., M. Lagueux, PVF2, a PDGF/VEGF-like growth factor, induces hemocyte proliferation in *Drosophila* larvae. *EMBO Rep.* **3**, 1195–1200 (2002).

63. S. G. Tattikota, B. Cho, Y. Liu, Y. Hu, V. Barrera, M. J. Steinbaugh, S. H. Yoon, A. Comjean, F. Li, F. Dervis, R. J. Hung, J. W. Nam, S. Ho Sui, J. Shim, N. Perrimon, A single-cell survey of *Drosophila* blood. *eLife* **9**, e54818 (2020).
64. D. Bakopoulos, J. C. Whisstock, C. G. Warr, T. K. Johnson, Macrophage self-renewal is regulated by transient expression of PDGF- and VEGF-related factor 2. *FEBS J.* **289**, 3735–3751 (2022).
65. P. P, A. Tomar, S. Madhwal, T. Mukherjee, Immune control of animal growth in homeostasis and nutritional stress in *Drosophila*. *Front. Immunol.* **11**, 1528 (2020).
66. A. Defaye, I. Evans, M. Crozatier, W. Wood, B. Lemaitre, F. Leulier, Genetic ablation of *Drosophila* phagocytes reveals their contribution to both development and resistance to bacterial infection. *J. Innate Immun.* **1**, 322–334 (2009).
67. J. Colombani, L. Bianchini, S. Layalle, E. Pondeville, C. Dauphin-Villemant, C. Antoniewski, C. Carre, S. Noselli, P. Leopold, Antagonistic actions of ecdysone and insulins determine final size in *Drosophila*. *Science* **310**, 667–670 (2005).
68. C. Mirth, J. W. Truman, L. M. Riddiford, The role of the prothoracic gland in determining critical weight for metamorphosis in *Drosophila melanogaster*. *Curr. Biol.* **15**, 1796–1807 (2005).
69. N. Okamoto, N. Yamanaka, Nutrition-dependent control of insect development by insulin-like peptides. *Curr. Opin. Insect. Sci.* **11**, 21–30 (2015).
70. R. Delanoue, E. Meschi, N. Agrawal, A. Mauri, Y. Tsatskis, H. McNeill, P. Leopold, *Drosophila* insulin release is triggered by adipose Stunted ligand to brain Methuselah receptor. *Science* **353**, 1553–1556 (2016).
71. C. Geminard, E. J. Rulifson, P. Leopold, Remote control of insulin secretion by fat cells in *Drosophila*. *Cell Metab.* **10**, 199–207 (2009).
72. A. Rajan, N. Perrimon, *Drosophila* cytokine unpaired 2 regulates physiological homeostasis by remotely controlling insulin secretion. *Cell* **151**, 123–137 (2012).
73. N. Agrawal, R. Delanoue, A. Mauri, D. Basco, M. Pasco, B. Thorens, P. Leopold, The *Drosophila* TNF eiger is an adipokine that acts on insulin-producing cells to mediate nutrient response. *Cell Metab.* **23**, 675–684 (2016).
74. A. Ratheesh, V. Belyaeva, D. E. Siekhaus, *Drosophila* immune cell migration and adhesion during embryonic development and larval immune responses. *Curr. Opin. Cell Biol.* **36**, 71–79 (2015).
75. B. Parsons, E. Foley, The *Drosophila* platelet-derived growth factor and vascular endothelial growth factor-receptor related (Pvr) protein ligands Pvf2 and Pvf3 control hemocyte viability and invasive migration. *J. Biol. Chem.* **288**, 20173–20183 (2013).
76. I. A. Droujinine, N. Perrimon, Interorgan communication pathways in physiology: Focus on *Drosophila*. *Annu. Rev. Genet.* **50**, 539–570 (2016).
77. L. Gnessi, A. Emidi, D. Farini, S. Scarpa, A. Modesti, T. Ciampani, L. Silvestroni, G. Spera, Rat Leydig cells bind platelet-derived growth factor through specific receptors and produce platelet-derived growth factor-like molecules. *Endocrinology* **130**, 2219–2224 (1992).
78. L. Gnessi, A. Emidi, E. A. Jannini, E. Carosa, M. Maroder, M. Arizzi, S. Ulisse, G. Spera, Testicular development involves the spatiotemporal control of PDGFs and PDGF receptors gene expression and action. *J. Cell Biol.* **131**, 1105–1121 (1995).
79. K. L. Loveland, K. Zlatic, A. Stein-Oakley, G. Risbridger, D. M. deKretser, Platelet-derived growth factor ligand and receptor subunit mRNA in the Sertoli and Leydig cells of the rat testis. *Mol. Cell. Endocrinol.* **108**, 155–159 (1995).
80. C. C. Taylor, Platelet-derived growth factor activates porcine thecal cell phosphatidylinositol-3-kinase-Akt/PKB and ras-extracellular signal-regulated kinase-1/2 kinase signaling pathways via the platelet-derived growth factor-beta receptor. *Endocrinology* **141**, 1545–1553 (2000).
81. S. Basciani, S. Mariani, M. Arizzi, S. Ulisse, N. Rucci, E. A. Jannini, C. Della Rocca, A. Manicone, C. Carani, G. Spera, L. Gnessi, Expression of platelet-derived growth factor-A (PDGF-A), PDGF-B, and PDGF receptor-alpha and -beta during human testicular development and disease. *J. Clin. Endocrinol. Metab.* **87**, 2310–2319 (2002).
82. J. Brennan, C. Tilmann, B. Capel, Pdgfr-alpha mediates testis cord organization and fetal Leydig cell development in the XY gonad. *Genes Dev.* **17**, 800–810 (2003).
83. P. Soriano, Abnormal kidney development and hematological disorders in PDGF beta-receptor mutant mice. *Genes Dev.* **8**, 1888–1896 (1994).
84. P. Soriano, The PDGF alpha receptor is required for neural crest cell development and for normal patterning of the somites. *Development* **124**, 2691–2700 (1997).
85. J. Schmahl, K. Rizzolo, P. Soriano, The PDGF signaling pathway controls multiple steroid-producing lineages. *Genes Dev.* **22**, 3255–3267 (2008).
86. S. A. Sinenko, B. Mathey-Prevot, Increased expression of *Drosophila* tetraspanin, Tsp68C, suppresses the abnormal proliferation of ytr-deficient and Ras/Raf-activated hemocytes. *Oncogene* **23**, 9120–9128 (2004).
87. T. Ikeya, M. Galic, P. Belawat, K. Nairz, E. Hafen, Nutrient-dependent expression of insulin-like peptides from neuroendocrine cells in the CNS contributes to growth regulation in *Drosophila*. *Curr. Biol.* **12**, 1293–1300 (2002).
88. J. Colombani, S. Raisin, S. Pantalacci, T. Radimerski, J. Montagne, P. Leopold, A nutrient sensor mechanism controls *Drosophila* growth. *Cell* **114**, 739–749 (2003).
89. E. J. Rulifson, S. K. Kim, R. Nusse, Ablation of insulin-producing neurons in flies: Growth and diabetic phenotypes. *Science* **296**, 1118–1120 (2002).
90. M. Palomino-Schatzlein, J. Carranza-Valencia, J. Guirado, S. Juarez-Carreno, J. Morante, A toolbox to study metabolic status of *Drosophila melanogaster* larvae. *STAR Protoc.* **3**, 101195 (2022).
91. D. Rosin, E. Schejter, T. Volk, B. Z. Shilo, Apical accumulation of the *Drosophila* PDGF/VEGF receptor ligands provides a mechanism for triggering localized actin polymerization. *Development* **131**, 1939–1948 (2004).
92. M. J. Texada, A. Malita, C. F. Christensen, K. B. Dall, N. J. Faergeman, S. Nagy, K. A. Halberg, K. Rewitz, Autophagy-mediated cholesterol trafficking controls steroid production. *Dev. Cell* **48**, 659–671.e4 (2019).

Acknowledgments: We are indebted to the Bloomington Stock Center at Indiana University (Bloomington, IN) and the Vienna *Drosophila* Resource Center (VDRC) and to Dr. D. Siekhaus for sharing RNA-seq gene expression analysis of embryonic hemocytes, B. Shilo for the gift of rat anti-Pvr antibody, B. Lemaitre for the gift of UAS-pvf2 lines, S. Sinenko for the gift of *hmlΔ-gal4;UAS-2xeGFP*, N. Perrimon for the gift of *srp^{hemo}-gal4* line, and T. K. Johnson for the gift of pvf2$^{tra\text{-}gal4}$. We are also indebted to the members of the Geissmann lab for helpful discussion and to D. Siekhaus, M. Milan, M. Dominguez, C. Glass, and N. Cox for critical reading and review of the manuscript before submission. **Funding:** This work was supported by NIH/NCI P30CA008748 to MSKCC and by NIH/NIAID 1R01AI130345, NIH/NHLBI R01HL138090, Leducq transatlantic network of excellence, Ludwig Institute for Cancer Research basic immunology grant to F.G. S.J.-C. is the recipient of a CRI Irvington postdoctoral fellow (CRI award 3440). **Author contributions:** S.J.-C. and F.G. designed the study and wrote the manuscript. S.J.-C. performed all experiments. **Competing interests:** The authors declare that they have no competing interests. **Data and materials availability:** All data needed to evaluate the conclusions in the paper are present in the paper and/or the Supplementary Materials.

Submitted 7 February 2023
Accepted 17 August 2023
Published 20 September 2023
10.1126/sciadv.adh0589